

# First-Principles Study of Electronic Structure and Optical Properties of Silicon/Carbon Nanotube

Wenyu Wang<sup>1</sup>, Jiangang Xu<sup>1</sup>, Yunguang Zhang<sup>1\*</sup>, Guixia Li<sup>2</sup>

<sup>1</sup>School of Science, Xi'an University of Posts and Telecommunications, Xi'an, China

<sup>2</sup>School of Science, China University of Petroleum, Qingdao, China

Email: \*zygsr2010@163.com

**How to cite this paper:** Wang, W.Y., Xu, J.G., Zhang, Y.G. and Li, G.X (2017) First-Principles Study of Electronic Structure and Optical Properties of Silicon/Carbon Nanotube. *Computational Chemistry*, 5, 159-171.

<https://doi.org/10.4236/cc.2017.54013>

**Received:** September 21, 2017

**Accepted:** October 24, 2017

**Published:** October 27, 2017

Copyright © 2017 by authors and Scientific Research Publishing Inc. This work is licensed under the Creative Commons Attribution International License (CC BY 4.0).

<http://creativecommons.org/licenses/by/4.0/>



Open Access

## Abstract

A supercell of a nanotube formed by a carbon nanotube (CNT) and a silicon nanotube (SiNT) is established. The electronic structure and optical properties are implemented through the first-principles method based on the density functional theory (DFT) with the generalized gradient approximation (GGA). The calculated results show that (6, 6) - (6, 6) silicon/carbon nanotubes (Si/CNTs) presented a direct band gap of 0.093 eV, (4, 4) - (6, 6) silicon/carbon nanotubes presented a direct band gap of 0.563 eV. The top of valence band was fundamentally determined by the Si-3p states and C-2p states, and the bottom of conduction band was primarily occupied by the C-2p states and Si-3p states in the Si/CNTs. It was found that (6, 6) - (6, 6) Si/CNTs have smaller energy band gap and better conductivity. Besides, Si/CNTs have satisfactory absorption characteristics and luminous efficiency in ultraviolet band.

## Keywords

Nanotubes, Electronic Structure, Optical Properties, First-Principles

## 1. Introduction

The discovery of CNTs since 1991 [1] have led to extensive research interest in one dimensional nanometer materials due to their unique properties and potential of applications [2] [3] [4] [5]. Recently, there has been a rapid growth research interests in advanced nanotechnology which gives great promise for achieving new sensing materials including high performance nanomaterials [6] and nanoscale electronics devices [7]. Silicon, as the same group element with carbon in the periodic table of elements has similar structure with carbon, and

has become one of hotspots in the field of nanometer materials research in recent years. Compared to other nanomaterials, SiNTs have more unique conduction properties. In addition, SiNTs have smaller size and excellent electrical properties, which enjoy broad application prospects in microelectronics and medicine and other fields. Some experimental researchers have attempted to develop the synthesis of SiNTs by a number of method such as chemical vapor deposition (CVD) method [8], template combined CVD [9]. In terms of theory, Luo *et al.* [10] studied the structures and electronic properties of pure (5, 5) and (5, 0) SiNTs with the first principles of density functional method, and found that the conductivity of SiNTs was connected with the chirality of its structure. According to the existing research findings [11], which shows that (n, 0) zigzag and (n, n) armchair SiNTs having  $n \geq 6$  are stable but those with  $n < 6$  can be stabilized by internal or external adsorption of transition metal elements. Therefore, there are a lot of researches on SiNTs [12]. For example, Yang *et al.* [13] observed the electronic structure and the changes of optical properties by applying different degrees of pre-tension deformation on single-wall armchair (6, 6) SiNTs through density functional theory. Referring to other researches, as for single-walled armchair SiNTs, doping P can make the energy band gap narrow, enhance electrical conductivity [14], and doping Al can increase the optical absorption bandwidth of SiNTs, and improve the photoelectric properties [15]. Additionally, the SiNTs of different chirality have different levels of thermal stability, electrical conductivity and energy performance [16] [17]. With the further research work, more special nanotubes have been studied [18] [19]. A coaxial cylindrical heterojunction of carbon tubes, which consists of alternant bands of 5- and 7-membered rings, can be formed by one armchair (n, n) CNT and one zigzag (2n, 0) CNT. The torsional mechanical properties are studied by using molecular dynamics method [20]. People have made some researches on the structure and properties of SiNTs, but few involve Si/CNTs. In the present paper, the electronic structure and optical properties of (4, 4) - (6, 6) Si/CNTs and (4, 4) - (6, 6) Si/CNTs are studied.

In the present work, the electronic properties of Si/CNTs formed by a CNT and a SiNT are investigated with the method of the first-principles density functional theory. In the following, we first investigated electronic properties of Si/CNTs in terms of energy band and density of states (DOS). And then the simulation results of optical properties of Si/CNTs are studied in Section 3. Finally, we conclude in Section 4. This work provided a theoretical basis for the application of SiNTs in photoelectric device.

## 2. Simulation Model and Method

### 2.1. Model

To study the structural feature and the electronic property of (6, 6) - (6, 6) Si/CNTs and (4, 4) - (6, 6) Si/CNTs, supercell are established. Periodic armchair nanotubes which both ends were not closed and infinitely long were adopted.

Calculation was conducted on  $a \times a \times c$  orthogonal supercell, and nanotubes infinitely extended along the repeating units of heterostructure at the direction  $c$ . In Si/CNTs structure, SiNTs and CNTs occupied half in the heterostructure along the axial direction. Parameter and constant of supercell are set as  $1 \times 1 \times 4$ ,  $\alpha = \beta = 90^\circ$ ,  $\gamma = 120^\circ$ , respectively. (6, 6) - (6, 6) Si/CNTs include 48 Si atoms and 48 C atoms. (4, 4) - (6, 6) Si/CNTs include 32 Si atoms and 48 C atoms (ref. **Figure 1**).

## 2.2. Method

In this work, the first principles calculations for the computational method were carried out using CASTEP package to perform geometry optimization and the specific properties such as band energy and density of states (DOS). All the relaxation and electronic calculations were performed based on the DFT, within the Perdew-Burke-Ernzerhof (PBE) formulation of the generalized gradient approximation [21]. The convergence criteria for total energy and the cutoff energy of the plane-wave basis are set as  $1.0 \times 10^{-6}$  eV and 400 eV. Integration on the Brillouin zone is performed using special  $k$  points generated by the Monkhorst-Pack [22] grid with the value of  $1 \times 1 \times 1$ ,  $1 \times 1 \times 1$ ,  $2 \times 1 \times 1$  for SiNTs, (6, 6) - (6, 6) Si/CNTs and (4, 4) - (6, 6) Si/CNTs, respectively. Energy calculations were carried out in the reciprocal space. The valence electron states of all atoms considered:  $C2s^22p^2$ ,  $Si3s^23p^2$ .

## 3. Results and Discussion

### 3.1. Geometry Optimized

In order to make the model energy tend to be stable, and more close to the real material, and ensure that parameters used in the simulation get accurate results, the initial model was first optimized. The geometry of the (6, 6) SiNTs, (6, 6) - (6, 6) Si/CNTs and (4, 4) - (6, 6) Si/CNTs are optimized by using a Broyden-Fletcher-Goldfarb-Shanno (BFGS) minimizer [23]. Optimization accuracy is set as Fine. The optimized lattice parameters and structure of SiNTs and Si/CNTs are shown in **Table 1** and **Figure 2**.

**Table 1.** Optimized lattice parameters of (6, 6) SiNT, (6, 6) - (6, 6) Si/CNT and (4, 4) - (6, 6) Si/CNT.

Type	optimized	a/Å	b/Å	c/Å	$d_{Si-Si}/\text{Å}$	$d_{C-C}/\text{Å}$	$d_{C-Si}/\text{Å}$
(6, 6) SiNT	before	16.7542	16.7542	16.2120	2.34	-	-
	after	15.7315	15.2161	15.6251	2.261	-	-
(6, 6) - (6, 6) Si/CNT	before	16.4104	16.4104	15.7963	2.34	1.42	-
	after	12.3433	12.3375	13.7579	2.362	1.431	1.895
(4, 4) - (6, 6) Si/CNT	before	12.0560	12.0560	15.7963	2.34	1.42	-
	after	11.3745	12.3977	12.4007	2.370	1.421	1.882

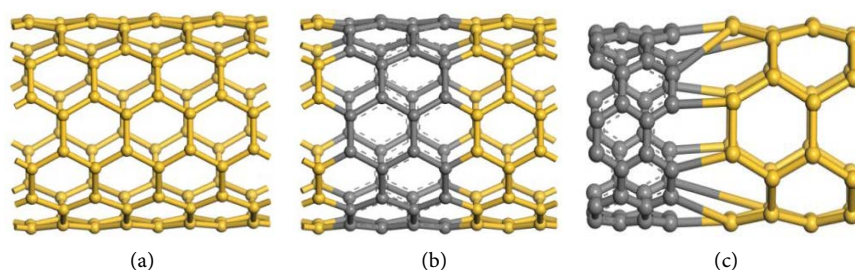


**Figure 1.** Structure schematics of (6, 6) SiNT, (6, 6) - (6, 6) Si/CNT and (4, 4) - (6, 6) Si/CNT (The yellow ball: silicon atom; The grey ball: carbon atom). (a) (6, 6) SiNT; (b) (6, 6) - (6, 6) Si/CNT; (c) (4, 4) - (6, 6) Si/CNT.

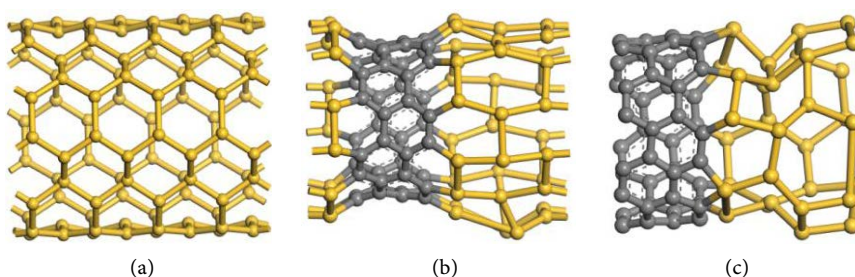


**Figure 2.** Optimized structure schematics of (6, 6) SiNT, (6, 6) - (6, 6) Si/CNT, and (4, 4) - (6, 6) Si/CNT. (a) (6, 6) SiNT; (b) (6, 6) - (6, 6) Si/CNT; (c) (4, 4) - (6, 6) Si/CNT.

In the process of optimization, the change of internal bond length and bond angle of nanotubes changed the cell volume, but the optimized Si/CNTs crystal cell parameters were close. Si-Si bond in SiNTs has bigger length fluctuation and lower chemical displacement degree. Compared with the smooth structure of CNTs surface, the surface of SiNTs appeared folding structure, and Si/CNTs surface presented some deformation. By comparing with the model in **Figure 1**, it showed that optimization had a greater influence on SiNTs, while slightly affected CNTs part.

### 3.2. Electronic Structures

To have a understanding of the electronic properties of Si/CNTs, the band structure and DOS for the single-walled armchair (6, 6) SiNTs, (4, 4) - (6, 6) Si/CNTs and (6, 6) - (6, 6) Si/CNTs were calculated and presented in **Figures 3-5**. **Figure 3(a)** shows the band structure of the single-walled armchair (6, 6) SiNTs. The bottom of the conduction band of the nanotube locates at the G point of its Brillouin zone, and the top of valence band lies between the point G and F. Besides, the coordinate of them are (0, 0) and (0.14, 0), respectively, indicating that the nanotubes is an indirect gap semiconductor. The obtained band gap is 0.314 eV, which is highly in consistent with the result of Yang's [24].

The valence band of (6, 6) SiNTs mainly comprises the lower valence band of -12 eV - 5 eV and upper valence band of -5 eV - 0 eV. The top of valence band was fundamentally determined by the Si-3p states and the bottom of conduction band was primarily occupied by the Si-3s states and Si-3p states, showing that

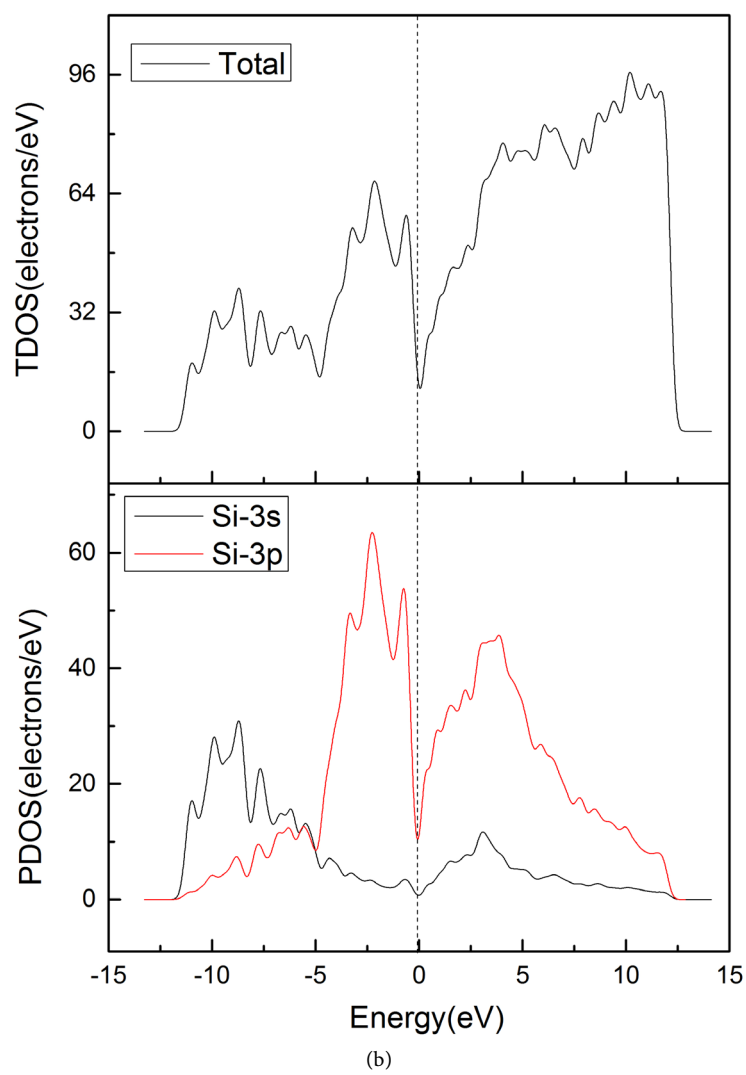
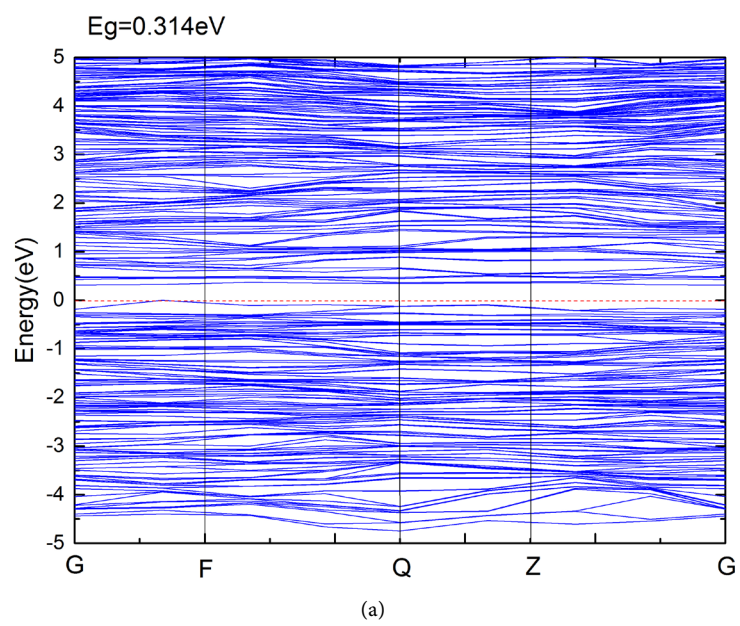


**Figure 3.** Band structure (a) and density of states (b) of silicon nanotube.

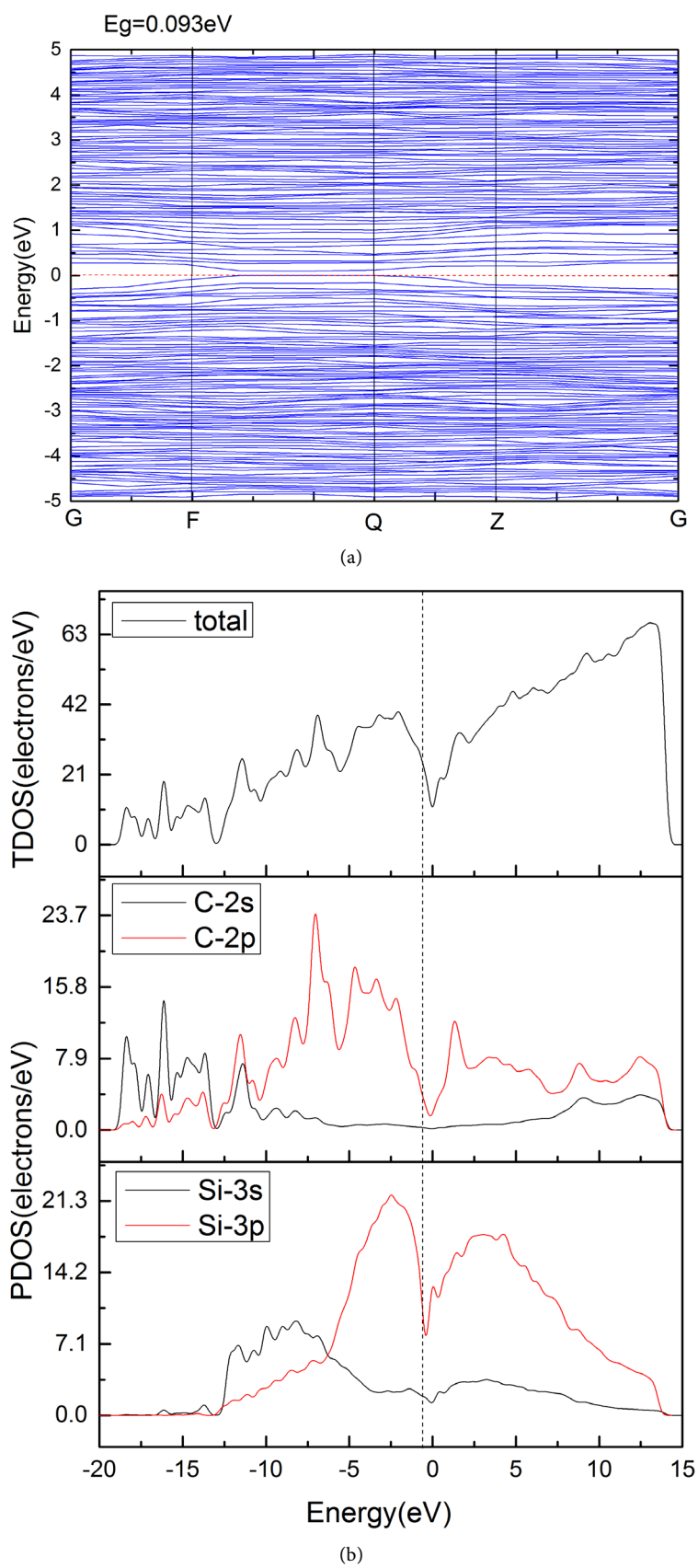


**Figure 4.** Band structure (a) and density of states (b) of (6, 6) - (6, 6) Si/CNT.

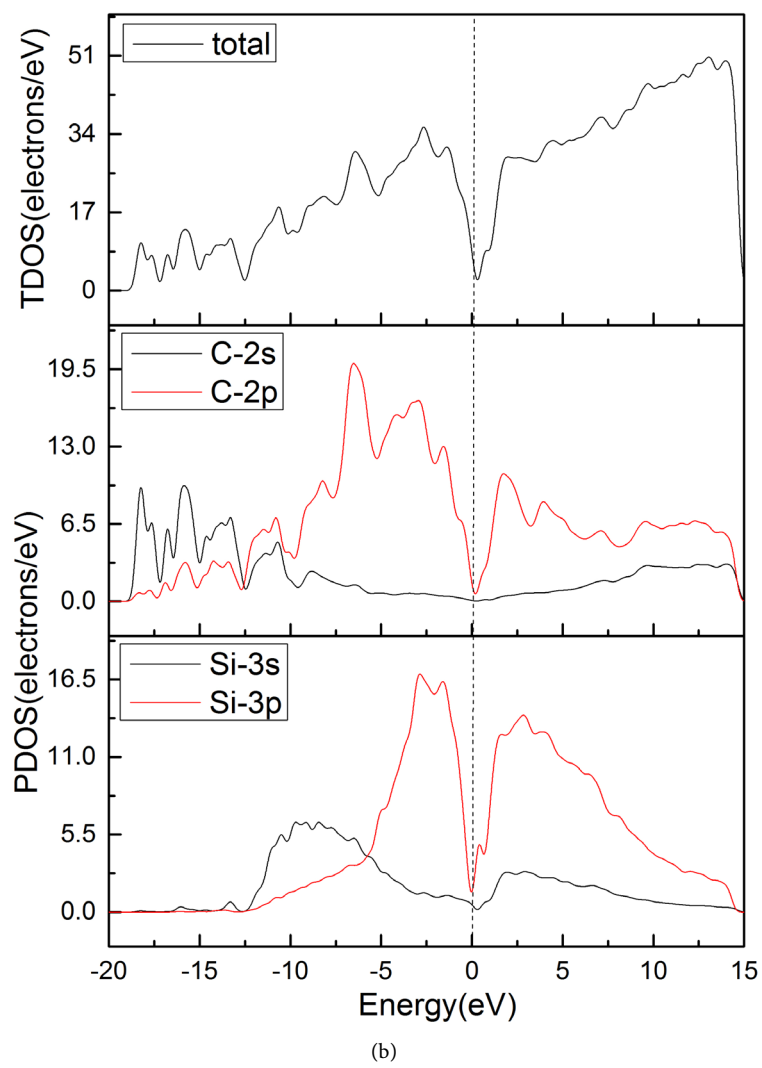
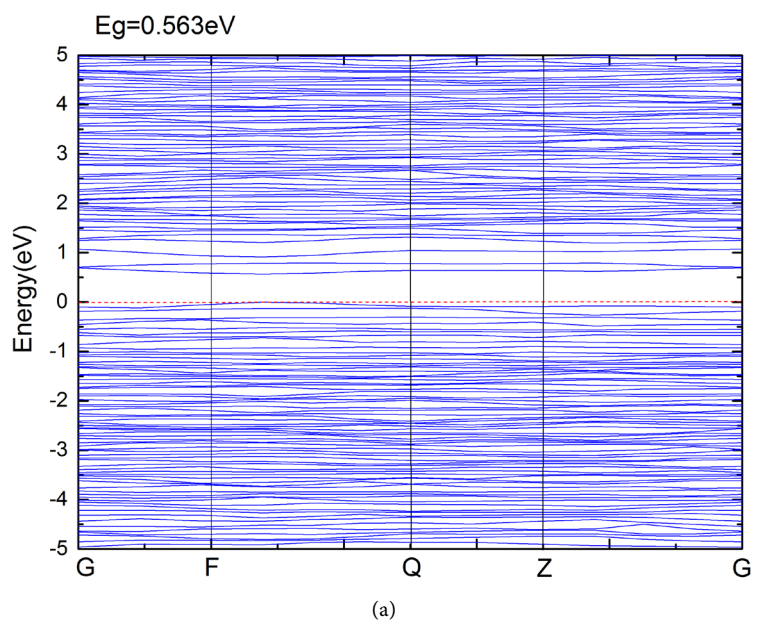


**Figure 5.** Band structure (a) and density of states (b) of (4, 4) - (6, 6) Si/CNT.

the bonding is mainly formed by *sp* hybridization. In distant region far from Fermi level, the *sp* hybridization of *s* electrons and *p* electrons for SiNTs relatively remains obvious. The lower valence band is mainly formed from Si-3s states, in which the Si-3p states exert a weak influence. Besides, the upper valence band mainly originates from Si-3p states.

**Figure 4** and **Figure 5(a)** point out that the Si/CNTs exhibit semiconductor with small band gaps, less than 1 eV. The (6, 6) - (6, 6) Si/CNTs have a direct band gap of 0.093 eV (**Figure 4(a)**), which is narrower than that of single-walled armchair (6, 6) SiNTs. The bottom of the conduction band and the top of valence band of the nanotube are located between the point F and Q of its Brillouin zone. With the top of valence band and the bottom of the conduction band between the point F and Q, the (4, 4) - (6, 6) Si/CNTs make a direct band gap of 0.563 eV, which is larger than that of (6, 6) SiNTs.

To make further study on the electronic structure of Si/CNTs, the partial density of states (PDOS) of C atoms and Si atoms in the nanotube section are investigated (in **Figure 4** and **Figure 5(b)**). The PDOS for (4, 4) - (6, 6) Si/CNTs are similar. Based on the curve, it can be seen that the bottom of the conduction band and the top of valence band are occupied by Si-3p states and C-2p states, in which the Si-3s states make a weak influence. As it shows, near the Fermi level and in the high energy region, about from -5 eV - 5 eV, the quantity of split energy levels for Si/CNTs all decrease to some extent compared with SiNTs. Besides, the bonding is mainly formed by interaction of C-2p states and Si-3p electronic states. However, in the low energy region of valence band (left of the Fermi level), about from -20 eV - -5 eV, as certain band width exists between C-2s states and C-2p states, Si-3s states and Si-3p states, yet is mainly from the interaction among *s* electrons. However, the action of *p* electrons is relatively weaker, which exhibits *sp* hybridization. In particular, the figure also shows that compared with (6, 6) - (6, 6) Si/CNTs, the hybridization strength of (4, 4) - (6, 6) Si/CNTs decrease slightly, and density peak strength of total electronic state is all weakened, indicating that the interelectronic locality for (4, 4) - (6, 6) Si/CNTs is relatively weaker. In the vicinity of Fermi level, the peak shape of Si/CNTs is basically similar, with key distinction being caused by the changes of Si-3p electrons near Fermi level.

### 3.3. Dielectric Function and Absorption

According to the law of electron transition and Kramers-Kronig dispersion relation [25], the complex dielectric and optical properties are calculated, using the well-known relation:

$$\varepsilon(\omega) = \varepsilon_1(\omega) + i\varepsilon_2(\omega) \quad (1)$$

The real part of the dielectric function follows from the relation:

$$\varepsilon_1(\omega) = 1 + \frac{8\pi^2 e^2}{m^2} \cdot \sum_{v,c} \int_{BZ} d^3K \frac{2}{(2\pi)} \times \frac{|e \cdot M_{cv}(K)|^2}{[E_c(K) - E_v(K)]} \quad (2)$$

The imaginary part  $\varepsilon_2(\omega)$ , in the long wavelength limit, has been obtained directly from the electronic structure calculation:

$$\varepsilon_2(\omega) = \frac{4\pi^2}{m^2\omega^2} \cdot \sum_{v,c} \int_{BZ} d^3K \frac{2}{(2\pi)} \times |e \cdot M_{cv}(K)|^2 \times \delta[E_c(K) - E_v(K) - \hbar\omega] \quad (3)$$

$M_{cv}(K)$  are the transition moments elements.

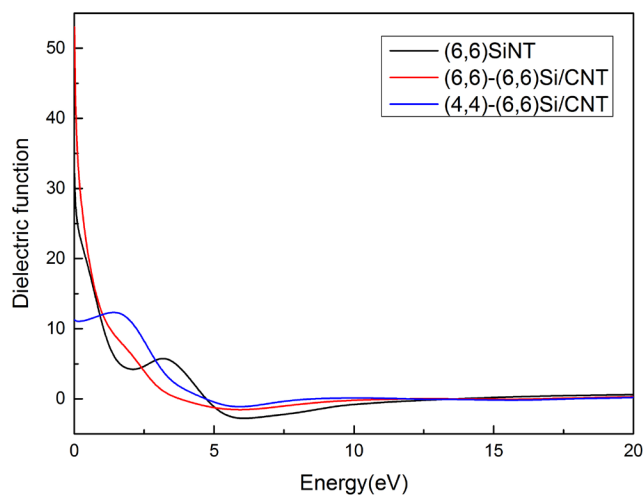
The absorption coefficient is given by the following relation:

$$\alpha(\omega) = \sqrt{2}\omega \left[ \sqrt{\varepsilon_1^2(\omega) + \varepsilon_2^2(\omega)} - \varepsilon_1(\omega) \right]^{1/2} \quad (4)$$

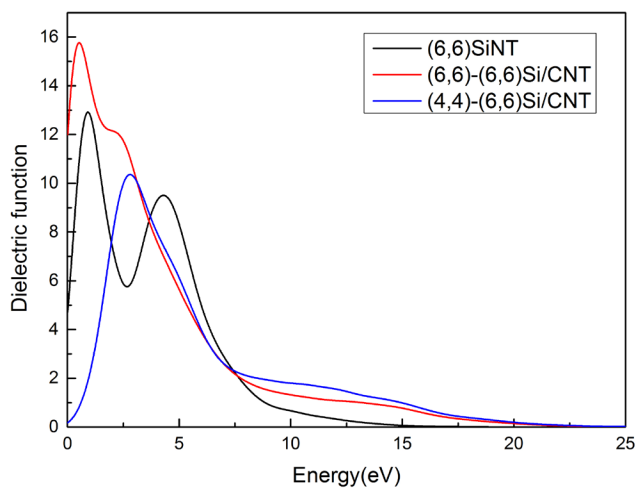
$\hbar, \omega, K$  are Planck constant, the angular frequency and reciprocal vector, respectively. Subscript C and V represent the conduction band and the valence band of nanotubes, and BZ is the first Brillouin zone.  $E_c(K)$  and  $E_v(K)$  represent the intrinsic level of the conduction band and the valence band.  $|e \cdot M_{cv}(K)|^2$  is Momentum transition matrix element of Transition electrons.

To further analyze the optical properties for the two types of Si/CNTs, **Figure 6** and **Figure 7** presents the real part and the imaginary part of dielectric function and absorption for single-wall armchair (6, 6) SiNTs, (6, 6) - (6, 6) Si/CNTs and (4, 4) - (6, 6) Si/CNTs. **Figure 6(a)** presents that the static dielectric constant for single-wall armchair (6, 6) SiNTs is 32.188, and a dielectric absorption peak appears near 3.307 eV with increase of energy. The static dielectric constants of (6, 6) - (6, 6) Si/CNTs and (4, 4) - (6, 6) Si/CNTs are 53.043 and 11.281, respectively, which also shows that a dielectric absorption peak appears when the energy of (4, 4) - (6, 6) Si/CNTs increases to near 1.547. According to the inversely proportional relationship between the dielectric constant and the energy gap width of semiconductor materials, the dielectric constant of (6, 6) - (6, 6) Si/CNTs increase as its energy gap width decreases, while the dielectric constant of (4, 4) - (6, 6) Si/CNTs decrease as its energy gap width increases. This result is consistent with the calculations of energy band structure. Analysis finds that the structure of Si/CNTs can change the dielectric absorption width of real part of SiNTs.

**Figure 6(b)** presents the imaginary part of dielectric function of SiNTs and Si/CNTs are presented in. Based on the figure, a sharp maximal dielectric peak in imaginary part of dielectric function for SiNTs appears in the vicinity of 0.959 eV, which is mainly caused by intrinsic transition among Si-3p and Si-3s electrons. Besides, with the increase of energy, the dielectric peak in imaginary part appears in the vicinity of 4.359 eV and tapers. In terms of the (6, 6) - (6, 6) Si/CNTs, the dielectric peak strength of in low energy region increases, and conductivity is enhanced. With the increase of energy, a maximum dielectric peak appears in the vicinity of 0.443 eV which declined. Then, a small dielectric peak appears in the vicinity of 2.243 eV. While the strength of dielectric peak for (4, 4) - (6, 6) Si/CNTs is weakened to some extent, with a dielectric absorption peak appearing in the vicinity of 2.784 eV, indicating that the structure of Si/CNTs can change the dielectric absorption width in imaginary part of SiNTs, and (6, 6) - (6, 6) Si/CNTs has higher conductivity.



(a)



(b)

**Figure 6.** Dielectric function of (6, 6) SiNT, (6, 6) - (6, 6) Si/CNT and (4, 4) - (6, 6) Si/CNT. (a) Real part; (b) imaginary part.

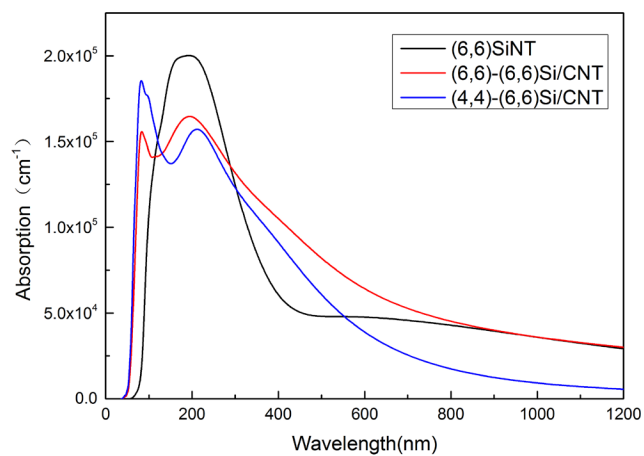


**Figure 7.** Absorption spectra of (6, 6) SiNT, (6, 6) - (6, 6) Si/CNT and (4, 4) - (6, 6) Si/CNT.

The calculate absorption coefficient of SiNTs and Si/CNTs are provided in **Figure 7**. Strong absorption peak appears between 100 nm - 400 nm for absorption of (6, 6) SiNTs, and calculate absorption is above  $1.5 \times 10^5 \text{ cm}^{-1}$ , proving SiNTs have good absorption characteristics in far ultraviolet band and near ultraviolet band. In addition, the figure also shows that the absorption spectrums for (6, 6) - (6, 6) Si/CNTs and (4, 4) - (6, 6) Si/CNTs all have strong absorption peak at 100 nm - 200 nm and 200 nm - 400 nm, indicative of good absorption characteristics of Si/CNTs in the ultraviolet band, and the optical absorption band width of Si/CNTs is large in the high energy region near 70 nm - 120 nm, photoabsorption characteristics of far ultraviolet band is satisfactory. Besides, within 120 nm - 300 nm, the absorption coefficients of Si/CNTs all declines compared with (6, 6) silicon nanotube. However, absorption coefficient represents the attenuation percentage of light intensity in unit propagation length in nanotubes, so luminous efficiency of the Si/CNTs increases.

#### 4. Conclusion

To conclude, in this paper, we perform first-principles calculations in the framework of density-functional theory to determine the electronic structure and optical properties of single-walled armchair (6, 6) SiNTs, (6, 6) - (6, 6) Si/CNTs and (4, 4) - (6, 6) Si/CNTs. The calculated results indicate that (6, 6) SiNTs is an indirect band gap of 0.314 eV. The (6, 6) - (6, 6) Si/CNT is a direct-gap semiconductor with band gap of 0.093 eV, and (4, 4) - (6, 6) Si/CNT is a direct-gap semiconductor with energy gap of 0.563 eV. The top of valence band of Si/CNTs is mainly determined by Si-3p and C-2p electrons, and the bottom of conduction band is occupied by the C-2p electrons, Si-3p electrons and a small amount of Si-3s electrons. It shows that the (6, 6) - (6, 6) Si/CNTs has smaller band gap and higher conductivity, and (6, 6) - (6, 6) Si/CNTs and (4, 4) - (6, 6) Si/CNTs have satisfactory absorption characteristics in ultraviolet band. Moreover, the results also provide instructive theoretical guidance for the applications of silicon nanotubes in optical detectors.

#### References

- [1] Iijima, S. (1991) Helical Microtubules of Graphitic Carbon. *Nature*, **354**, 56-58. <https://doi.org/10.1038/354056a0>
- [2] Sammalkorpi, M., Krashennnikov, A., Kuronen, A., Nordlund, K. and Kaski, K. (2004) Mechanical Properties of Carbon Nanotubes with Vacancies and Related Defects. *Physical Review B*, **70**, 121-127. <https://doi.org/10.1103/PhysRevB.70.245416>
- [3] Hou, W. and Xiao, S. (2007) Mechanical Behaviors of Carbon Nanotubes with Randomly Located Vacancy Defects. *Journal of Nanoscience & Nanotechnology*, **7**, 4478-4485. <https://doi.org/10.1166/jnn.2007.862>
- [4] Kinoshita, Y., Murashima, M., Kawachi, M. and Ohno, N. (2013) First-Principles Study of Mechanical Properties of One-Dimensional Carbon Nanotube Intramolecular Junctions. *Computational Materials Science*, **70**, 1-7. <https://doi.org/10.1016/j.commatsci.2012.12.033>

- [5] Chowdhury, S.C., Haque, B.Z. and Jr, J.W.G. (2014) Molecular Simulations of the Carbon Nanotubes Intramolecular Junctions under Mechanical Loading. *Computational Materials Science*, **82**, 503-509. <https://doi.org/10.1016/j.commatsci.2013.10.025>
- [6] Pandyan, K., Seenithurai, S. and Mahendran, M. (2012) Carbon Monoxide Adsorption on Transition Element-Doped Single Wall Carbon Nanotube. *Indian Journal of Physics*, **86**, 677-680. <https://doi.org/10.1007/s12648-012-0117-z>
- [7] Bistamam, M.S.A. and Azam, M.A. (2014) Tip-Growth of Aligned Carbon Nanotubes on Cobalt Supported by Alumina Using Alcohol Catalytic Chemical Vapor Deposition. *Result in Physics*, **4**, 105-106. <https://doi.org/10.1016/j.rinp.2014.07.003>
- [8] Li, C., Liu, Z.T., Gu, C., Xu, X. and Yang, Y. (2010) Controllable Synthesis and Growth Model of Amorphous Silicon Nanotubes with Periodically Dome-Shaped Interiors. *Advanced materials*, **18**, 228-234.
- [9] Sha, J., Niu, J.J. and Ma, X.Y. (2002) Silicon Nanotubes. *Advanced Materials*, **14**, 1219-1221.
- [10] Luo, Q., Zhang, Q., Zhang, Z., Tang, B. and Ran, Z. (2012) First Principle Study on the Structure and Electronic Property of Si Nanotubes. *Micronanoelectronic Technology*, **49**, 152-155.
- [11] Durgun, E., Tongay, S. and Ciraci, S. (2005) Silicon and III-V-Compound Nanotubes: Structure and Electric Properties. *Physical Review B*, **72**, Article ID: 075420. <https://doi.org/10.1103/PhysRevB.72.075420>
- [12] Lin, X., Lu, J.Z., Liu, J., Tang, Y.C. and Zhu, H.J. (2017) The Growth Model and Electronic Properties of Single- and Double-Walled Zigzag Silicon Nanotubes: Depending on the Structures. *Chemical Physics*, **483-484**, 156-164. <https://doi.org/10.1016/j.chemphys.2016.11.016>
- [13] Yang, Z.H., Liu, G.L., Qu, Y.D. and Li, R.D. (2015) Study on Electronic Structure and Optical Properties of Silicon Nanotube with Tensile Deformation. *Journal of Synthetic Crystals*, **44**, 2507-2512.
- [14] Yu, Z.Q., Zhang, C.H. and Lang, J.X. (2014) The Electronic Structure and Optical Properties of P-Doped Silicon Nanotube. *Acta Physica Sinica*, **63**, Article ID: 067102.
- [15] Zhang, C.H., Yu, Z.Q., Lang, J.X. and Liao, H.H. (2016) Electronic Structure and Photoelectric Properties of Al-Doped Single-Walled Armchair (6, 6) Silicon Nanotubes from First-Principles. *Material Review*, **30**, 147-151.
- [16] Barnard, A.S. and Russo, S.P. (2003) Structure and Energetics of Single Walled Armchair and Zigzag Silicon Nanotubes. *Journal of Physical Chemistry B*, **107**, 7577-7581. <https://doi.org/10.1021/jp0347421>
- [17] Fagan, S.B., Mota, R., Baierle, R.J., Paiva, G., Silva, A.J.R. and Fazzio, A. (2001) Stability Investigation and Thermal Behavior of a Hypothetical Silicon Nanotube. *Journal of Molecular Structure: THEOCHEM*, **539**, 101-106. [https://doi.org/10.1016/S0166-1280\(00\)00777-6](https://doi.org/10.1016/S0166-1280(00)00777-6)
- [18] Kang, Z., Li, M. and Tang, Q. (2010) Buckling Behavior of Carbon Nanotube-Based Intramolecular Junctions under Compression Molecular Dynamics Simulation and Finite Element Analysis. *Computational Materials Science*, **50**, 253-259. <https://doi.org/10.1016/j.commatsci.2010.08.011>
- [19] Li, M., Kang, Z., Yang, P., Meng, X. and Lu, Y. (2013) Molecular Dynamics Study on Buckling of Single-Wall Carbon Nanotube-Based Intramolecular Junctions and Influence Factors. *Computational Materials Science*, **67**, 390-396. <https://doi.org/10.1016/j.commatsci.2012.09.034>

- 
- [20] Han, D.R., Wang, L., Luo, C.L., Zhu, X.F. and Dai, Y.F. (2014) Torsional Mechanical Properties of (n, n)-(2n, 0) Carbon Nanotubes Heterojunction. *Journal of Magnetic Resonance*, **64**, 303-313.
- [21] Perdew, J.P., Burke, K. and Ernzerhof, M. (1996) Generalized Gradient Approximation Made Simple. *Physical Review Letters*, **77**, 3865. <https://doi.org/10.1103/PhysRevLett.77.3865>
- [22] Monkhorst, H.J. and Pack, J.D. (1976) Special Points for Brillouin Zone Integration. *Physical Review B*, **13**, 5188-5192. <https://doi.org/10.1103/PhysRevB.13.5188>
- [23] Broyden, C.G. (1970) The Convergence of a Class of Double Rank Minimization Algorithms II. The New Algorithm. *Journal of the Institute of Mathematics and Its Applications*, **6**, 222. <https://doi.org/10.1093/imamat/6.3.222>
- [24] Yang, X.B. and Ni, J. (2005) Electronic Properties of Single-Walled Silicon Nanotubes Compared to Carbon Nanotubes. *Physical Review B*, **72**, Article ID: 195426. <https://doi.org/10.1103/PhysRevB.72.195426>
- [25] Shen, X.C. (1992) *The Spectrum and Optical Property of Semiconductor*. Science Press, Beijing, 76.